

HfB₂ and Hf–B–N hard coatings by chemical vapor deposition

S. Jayaraman^{a,c}, J.E. Gerbi^{a,c}, Y. Yang^{a,c}, D.Y. Kim^{b,c}, A. Chatterjee^{a,c}, P. Bellon^{a,c},
G.S. Girolami^{b,c}, J.P. Chevalier^d, J.R. Abelson^{a,c,*}

^a Department of Materials Science and Engineering, University of Illinois at Urbana Champaign, 1304 W. Green Street, Urbana, IL-61801, USA

^b Department of Chemistry, University of Illinois at Urbana Champaign, 505 S. Mathews Avenue, Urbana, IL-61801, USA

^c Frederick Seitz Materials Research Laboratory, 104 S. Goodwin Avenue, Urbana, IL-61801, USA

^d Centre d'Etudes de Chimie Métallurgique, CNRS, 15, rue Georges Urbain, Vitry-sur-Seine 94407, France

Available online 27 December 2005

Abstract

Hard, dense and conformal hafnium diboride (HfB₂) thin films were obtained by CVD from the precursor Hf[BH₄]₄ at deposition temperatures ≤ 350 °C. As-deposited films were X-ray amorphous but transformed to a nanocrystalline structure after being annealed at 700 °C. Amorphous HfB₂ films exhibited a respectable hardness of 20 GPa; the hardness increased in the nanocrystalline state to 40 GPa. Ternary Hf–B–N films, which consisted of a mixture of HfB₂, HfN and BN were obtained by adding atomic nitrogen to the growth flux. The formation of the softer a-BN phase produced a drop in the hardness and modulus values. A multilayer HfB₂/Hf–B–N exhibited a good combination of high hardness (33 GPa) and low elastic modulus (300 GPa).

© 2005 Elsevier B.V. All rights reserved.

Keywords: Hafnium diboride; Hafnium borohydride; CVD; Hard coating; Nanoindentation; Nanocomposite

1. Introduction

Transition metal nitrides, carbides, borides and their mutual ternaries are popular materials for hard and environmental coatings [1–16]. Applications include cutting tools, wear resistant thin films and decorative coatings. Hafnium diboride (HfB₂) has a melting temperature of 3250 °C, a bulk hardness of 29 GPa and good corrosion resistance, properties that make it an excellent candidate for wear resistant coatings [17,18]. Despite such an attractive combination of properties, there are relatively few reports of transition metal boride thin films compared to transition metal nitrides. This situation can be traced to the processing difficulties associated with depositing boride films. Magnetron sputtering is a straightforward method to deposit such films, but stoichiometry control is a non-trivial issue [8]. Existing chemical vapor deposition (CVD) processes typically utilize halogenated precursors, e.g. TiCl₃ and BCl₃ to deposit TiB₂ [19–22], but corrosive gas handling and halogen contam-

ination of the films are significant disadvantages [23]. We present here an alternate CVD route to obtain hard, nanocrystalline HfB₂ thin films using the precursor tetrakis(tetrahydroborato)hafnium(IV) (hereafter, hafnium borohydride), Hf[BH₄]₄, at low process temperatures. We also produce Hf–B–N ternary alloys by adding atomic nitrogen to the growth flux and show how the final composition and hardness can be controllably modulated.

2. Experimental

HfB₂ thin films were grown by CVD from the precursor Hf[BH₄]₄. Growth was carried out in a UHV chamber described in detail elsewhere [24,25]. Films were deposited on various substrates including 20 mm × 12 mm Si (100) and 6 mm diameter, 0.4 mm thick molybdenum (Mo) discs. All the substrates were degreased in an ultrasonic bath in acetone, isopropyl alcohol and de-ionized water. Mo discs were mirror polished before degreasing. Silicon substrates were heated by flowing electric current through them; the temperature was measured with a pyrometer that had been calibrated against a thermocouple attached to the sample. Mo discs were attached to silicon with a ceramic adhesive and heated by thermal conduction. A 10–20

* Corresponding author. Department of Materials Science and Engineering, University of Illinois at Urbana Champaign, 1304 W. Green Street, Urbana, IL-61801, USA. Tel: +1 217 333 7258; fax: 1 217 244 2278.

E-mail address: abelson@uiuc.edu (J.R. Abelson).

°C temperature difference existed between the Mo and the underlying silicon in this arrangement, as measured by a thermocouple. A precursor pressure of 1.3×10^{-2} Pa (0.1 mTorr) was used for the present experiments. An argon–nitrogen mixture was dissociated in a remote plasma source consisting of a Pyrex tube in a microwave cavity [26]. The tube i.d. at its opening was 3.5 mm and it extended into the chamber ending ~ 13 cm from the substrate. Total chamber pressure during the growth of Hf–B–N films ranged from 0.49 to 0.85 Pa (3.7 to 6.4 mTorr) achieved by varying the amount of Ar–N₂ mixture. Ternary films were characterized by X-ray photoelectron spectroscopy (XPS) and also by Auger spectroscopy. The overlap of the peaks in Auger (Hf ~ 172 eV and B ~ 179 eV) made the absolute quantification of stoichiometry difficult. However, the relative atomic percentages for the ternary film could be obtained from the Auger sputter profile of a multilayer film consisting of nitrogen containing and nitrogen free layers. Film microstructures were analyzed by scanning (SEM) and transmission (TEM) electron microscopes and crystallinity characterized by X-ray diffraction (XRD). For plan-view TEM, films were deposited directly on a thin (~ 20 nm) SiO_x membrane supported by a copper grid. Film hardness (H) and reduced elastic modulus (E_r) were measured by nanoindentation using the procedure proposed by Oliver and Pharr [27,28]. The elastic modulus (E_f) was derived from the expression for the reduced modulus:

$$1/E_r = (1 - \nu_f^2)/E_f + (1 - \nu_i^2)/E_i$$

Poisson ratios for diamond ($\nu_i=0.07$), film ($\nu_f=0.25$) and the elastic modulus of diamond ($E_i=1141$ GPa) were used for the calculations. A typical loading profile consisted of multiple loading–unloading cycles with successively increasing loads to a maximum of 8 mN [29]. Indentation measurements were done on films in the thickness range 0.8–1 μm and the reported hardness values correspond to an indenter contact depth less than 10% of the film thickness. A Berkovich indenter was used for the tests and its tip area function was obtained by testing a standard quartz sample. The tip shape function was well-defined analytically for depths greater than 30 nm and the contact depth on our films well exceeded this value.

3. Results and discussion

3.1. HfB₂ microstructural control

The idealized growth reaction for the CVD growth process used here is $\text{Hf}[\text{BH}_4]_4 (\text{g}) \rightarrow \text{HfB}_2 (\text{s}) + \text{B}_2\text{H}_6 (\text{g}) + 5\text{H}_2 (\text{g})$. A substrate temperature of only 200 °C is needed for the onset of film growth [25]. A comparison of the representative film microstructures as a function of substrate temperature (T_s) illustrates the films grown at the high temperatures ($400^\circ\text{C} < T_s < 800^\circ\text{C}$) are columnar and not well densified (Fig. 1), which makes them unsuitable for hard coatings. This was observed for all films deposited between. We have shown that the columnar structure results from the high reaction probability of the incident precursor molecule [25]: the substrate tempera-

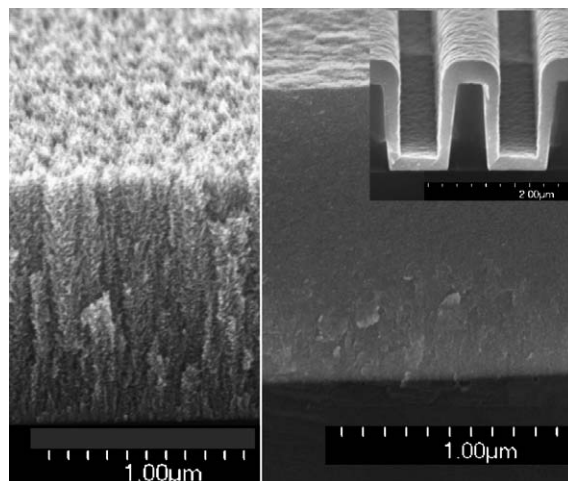


Fig. 1. SEM micrographs of fracture cross-sections: HfB₂ film deposited on Si at 600 °C (left), at 275 °C (right) and on trench structures in SiO₂ at 200 °C (right inset).

tures are too low ($T_s/T_{mp} < 0.3$) in all cases to allow for any substantial bulk or surface diffusion, processes that are needed to obtain dense and equiaxed grains in a physical vapor deposition process [30–32]. However, films deposited at low temperature (250–350 °C) appear dense and smooth due to a low precursor sticking coefficient; a high surface re-emission rate compensates for the lack of surface diffusion. Still, respectable growth rates of 10–50 nm/min accompanied by excellent step coverages are obtained in this regime (Fig. 1, inset).

Films deposited below 400 °C do not show any crystalline signature by XRD. Post-annealing in vacuum at $T \geq 600^\circ\text{C}$ for 60 min crystallizes the film, as is evident from the XRD profile (Fig. 2b). The broad and diffuse nature of the peaks suggests that the grains are small. Scherrer analysis on the peaks yielded an average grain size of 12 nm. Plan-view TEM of a similar film verifies that the film was nanocrystalline (Fig. 3). Interestingly, even the X-ray amorphous films contained some scattered crystallites as observed by the TEM. The post-annealed film showed a relatively uniform grain size distribution and only occasional large crystallites. Note that a nanocrystalline film can be grown at deposition temperatures of 500–600 °C, but a strong texture (Fig. 2a) and low film density renders the film useless for mechanical applications.

3.2. Hf–B–N alloys

A multiphase structure affords the possibility of reducing the modulus of the film while retaining its high hardness and wear resistance. Moreover, if the phases are immiscible, grain coarsening can be prevented and the nanostructure (and the consequent enhancement of mechanical properties) can be preserved during any subsequent thermal processing or operation under elevated temperature [10]. We added a flux of atomic nitrogen during film growth to produce N-containing phases. The remote plasma prevents the precursor from cracking, thus ensuring a low precursor sticking coefficient. A multilayer film served as a composition test structure. Here, the nitrogen

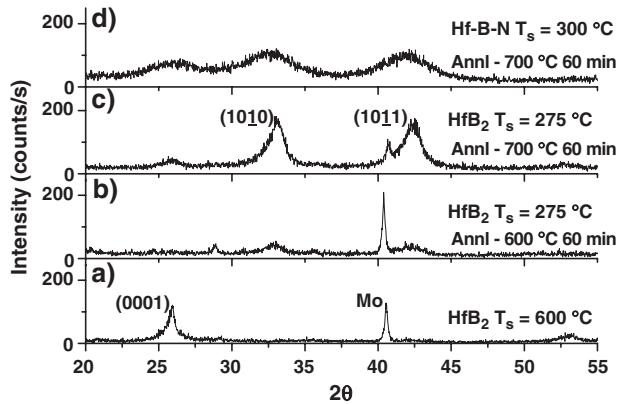


Fig. 2. XRD profiles of HfB_2 films deposited on Mo: (a) substrate temperature $T_s=600$ °C; (b) $T_s=275$ °C followed by annealing at 600 °C for 60 min; (c) $T_s=275$ °C followed by annealing at 700 °C for 60 min; (d) Hf–B–N film deposited on Si at 300 °C followed by annealing at 700 °C for 60 min.

content was modulated by switching the remote plasma on and off alternately. The Auger profile (Fig. 4a) shows that the nitrogen is incorporated only when the plasma is on, i.e. molecular N_2 is unreactive. The nitrogen replaces boron in the film but the hafnium content is almost unchanged. The oxygen content in the film bulk was <1 at.%. Also, the nitrogen content of the film is a function of the nitrogen flow rate when the plasma is on (Fig. 4b).

As-deposited Hf–B–N films are amorphous. Some crystallinity is observed by XRD after the films are annealed at 700 °C (Fig. 2d). Compared with HfB_2 annealed to the same temperature, the diffuse peaks here indicate a smaller crystal size or lower crystallinity, i.e. the presence of additional phases impeded the crystallization.

Sample transport in air from the growth chamber to the XPS chamber resulted in surface oxidation, but the amount of oxygen in the film bulk was below the instrumental detection

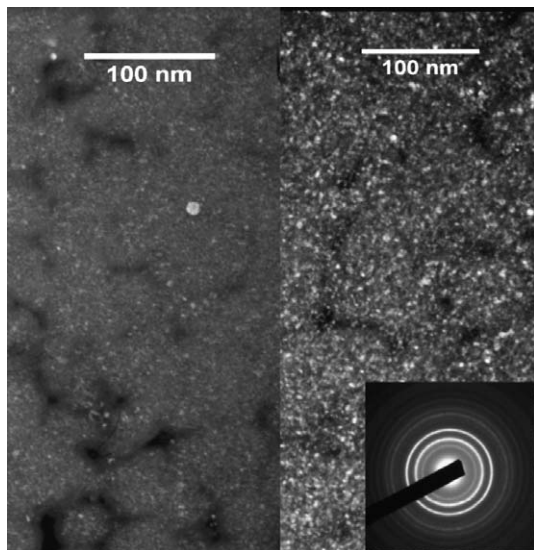


Fig. 3. Dark-field TEM image of a HfB_2 film deposited on SiO_x membrane/TEM copper grid at 275 °C, as deposited (left), post-annealed at 700 °C for 60 min (right) and the diffraction pattern from the annealed sample (inset).

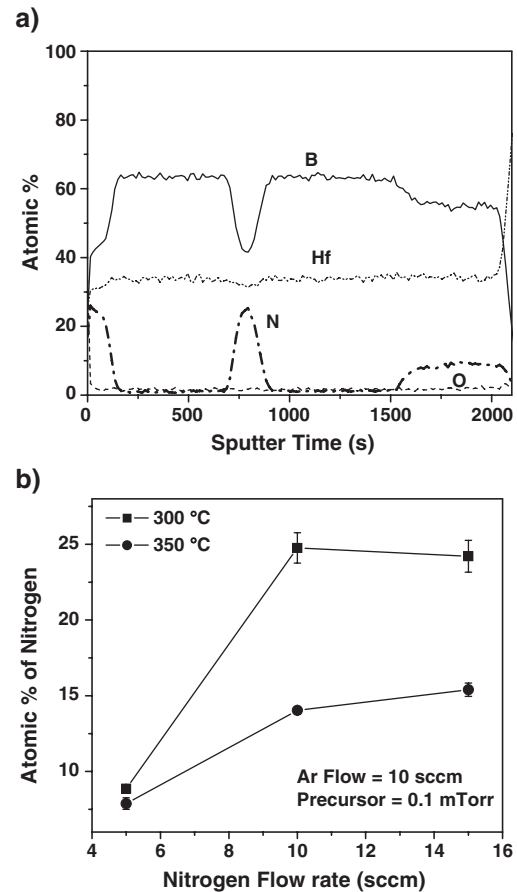


Fig. 4. Auger sputter depth profile from Hf–B–N films: (a) a multilayer film consisting of alternating HfB_2 and Hf–B–N layers; (b) film nitrogen content plotted vs. nitrogen flow rate for different substrate temperatures.

limits. Because sputtering typically causes preferential erosion of the lighter elements (boron and nitrogen) and phase mixing, we present here only a qualitative interpretation of the XPS data and do not attempt to quantify the phase composition. The Hf 4f peaks in Hf–B–N (15.2 and 16.8 eV) are midway between those of HfB_2 (14.7 eV and 16.3 eV) (Fig. 5a) and those for HfN (15.6 and 17.2 eV) [33]. The B peak has a poor signal-to-noise ratio due to the lower overall boron content in the Hf–B–N film, its preferential sputtering and a low sensitivity factor. Still, a shoulder at higher binding energy is apparent in this peak. The peak at 188.1 eV is similar to that observed in the HfB_2 film; the reported BN peak position at 191 eV is consistent with the observed shoulder [34]. The nitrogen 1s signal can be fitted with two peaks (397.3 and 399.2 eV) that are close to the reported values for nitrogen in HfN (397.6 eV) and BN (398 eV) [33,34]. From all these data, we conclude that the Hf–B–N films are a mixture of HfB_2 , HfN and BN.

3.3. Hardness

Dense homogeneous HfB_2 films were deposited at a substrate temperature of 275 °C on Mo discs for nanoindentation studies. The as-deposited amorphous HfB_2 film showed a respectable hardness of ~ 20 GPa (Fig. 6). For reference, we also measured an epitaxial TiN film on MgO , which yielded a

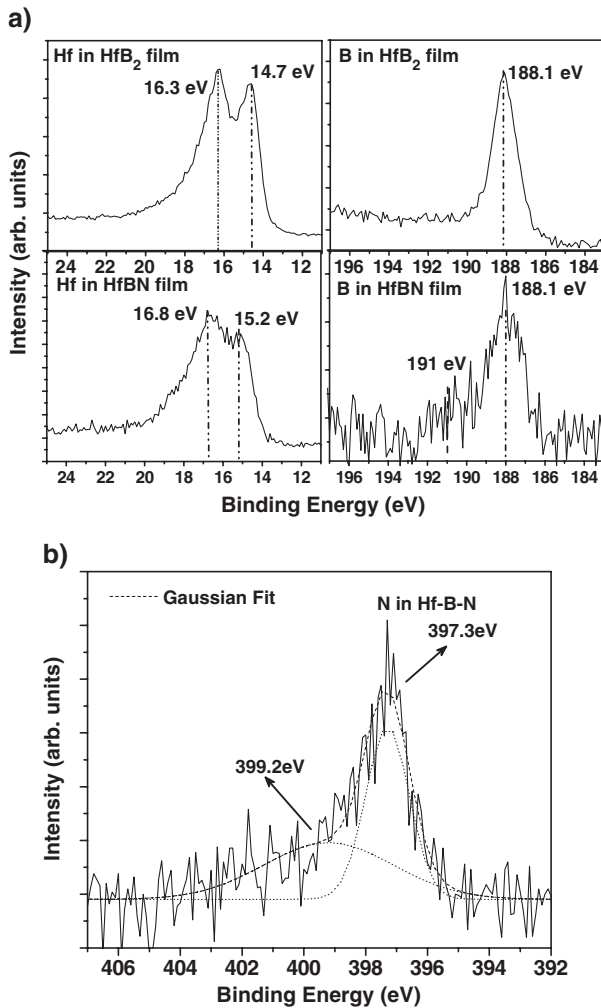


Fig. 5. XPS spectra of (a) Hf 4f and B 1s peaks from the HfB₂ and Hf-B-N films; (b) N 1s peak from the Hf-B-N film. See text for detailed interpretation.

hardness of ~ 20 GPa, similar to the literature value [14]. A HfB₂ film that was post-annealed at 600 °C had a hardness of 25 GPa; this film was not crystallized completely (Fig. 2b). The HfB₂ film post-annealed at 700 °C had a hardness of 40 GPa and an elastic modulus of 430 GPa. The hardness exceeds the

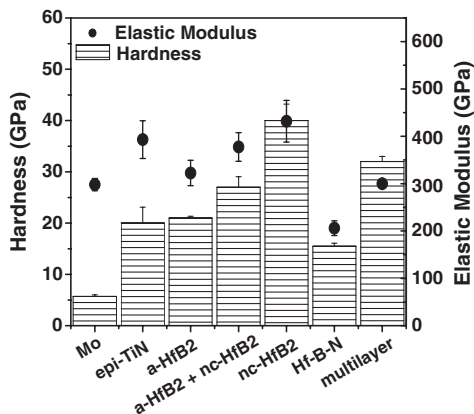


Fig. 6. Hardness and elastic modulus of the HfB₂ and Hf-B-N films from nanoindentation.

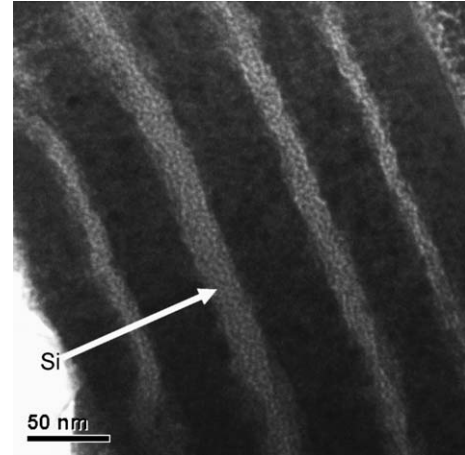


Fig. 7. Bright field cross-sectional TEM image from a HfB₂ (dark)/Hf-B-N (bright) multilayer film deposited at 300 °C Si and post-annealed at 700 °C for 60 min. The arrow on the figure indicates the direction of growth.

bulk value of 29 GPa [18], which is assumed to result from the nanometer sized grains in the film. The Hf-B-N films were significantly less hard ($H_f \sim 16$ GPa) and had lower modulus values ($E_f \sim 200$ GPa) than the monolithic HfB₂ films. We attribute this result to the formation of the softer amorphous BN phase and the lower film crystallinity. We also investigated the properties of a film consisting of alternating HfB₂ and Hf-B-N layers. A multilayered film was deposited on silicon from Hf[BH₄]₄ by growing the film with the plasma on for 2 min (~ 10 nm of Hf-B-N) followed by growing in the absence of atomic nitrogen for 2 min (~ 50 nm). The film was then post-annealed for 60 min at 700 °C. Auger depth profiles of annealed and unannealed multilayered films were identical within experimental error, suggesting that no significant inter-diffusion occurs during annealing. The annealed multilayered film has a lower elastic modulus ($E_f \sim 300$ GPa), but retains a relatively high hardness ($H_f \sim 33$ GPa). A bright field cross-sectional TEM image from an annealed multilayer film deposited on Si shows a lighter contrast for the nitrogen-containing layers compared to the nitrogen-free layers (Fig. 7). The contrast can be attributed to a lower crystallinity or the lower average Z of the ternary layer. It has been argued that the ratio H^3/E^2 is a better indicator than the hardness of the usefulness of the film for various applications [35]. The H^3/E^2 ratios for the HfB₂ and multilayer films are similar. The modulus of the latter implies, however, that our multilayered films are better matched elastically to common substrates such as Mo and steel, making them a promising candidate for wear related applications. Future studies will investigate the microstructure and phase composition of multilayer films in greater detail, with the aim of optimizing their mechanical properties.

4. Conclusions

A novel CVD process is used to obtain nanostructured hard HfB₂ films, free of halogen and organic contamination. The process affords high quality films at low deposition temperatures (~ 275 °C) and excellent step coverage. When the films

are deposited in the presence of atomic nitrogen from a remote N_2 plasma, the same process yields a multiphase ternary Hf–B–N film composed of HfB_2 , HfN and BN. The hardness (elastic modulus) values ranged from 15 GPa (200 GPa) for the ternary film to 40 GPa (430 GPa) for the post-annealed nanocrystalline HfB_2 film. We also prepared a multilayered composite structure consisting of alternating HfB_2 and Hf–B–N layers that had a combination of high hardness and low elastic modulus.

Acknowledgements

The authors are grateful to the National Science Foundation for support of this research under grant number NSF DMR-0354060 and Centre National de la Recherche Scientifique for support under a projet de cooperation. Compositional and structural analyses of the films were carried out in the Center for Microanalysis of Materials, University of Illinois, which is partially supported by the U.S. Department of Energy under grant DEFG02-91-ER45439. The authors also acknowledge H. S. Seo for providing epitaxial TiN reference sample for nanoindentation.

References

- [1] W. Gissler, Surf. Coat. Technol. 68 (1994) 556.
- [2] H. Karner, J. Laimer, H. Stori, P. Rodhammer, Surf. Coat. Technol. 39 (1989) 293.
- [3] P. Karvankova, M.G.J. Veprek-Heijman, O. Zindulka, A. Bergmaier, S. Veprek, Surf. Coat. Technol. 163 (2003) 149.
- [4] P.H. Mayrhofer, C. Mitterer, J. Musil, Surf. Coat. Technol. 174 (2003) 725.
- [5] C. Mitterer, M. Rauter, P. Rodhammer, Surf. Coat. Technol. 41 (1990) 351.
- [6] C. Mitterer, A. Ubleis, R. Ebner, Mater. Sci. Eng., A Struct. Mater.: Prop. Microstruct. Process. 140 (1991) 670.
- [7] C. Mitterer, P. Schmolz, H. Stori, Metall 48 (1994) 202.
- [8] C. Mitterer, J. Solid State Chem. 133 (1997) 279.
- [9] T.P. Mollart, J. Haupt, R. Gilmore, W. Gissler, Surf. Coat. Technol. 87-8 (1996) 231.
- [10] J. Patscheider, MRS Bull. 28 (2003) 180.
- [11] S. Veprek, S. Reiprich, Thin Solid Films 268 (1995) 64.
- [12] S. Veprek, M. Hausmann, S. Reiprich, L. Shizhi, J. Dian, Surf. Coat. Technol. 87-8 (1996) 394.
- [13] S. Veprek, Thin Solid Films 317 (1998) 449.
- [14] S. Veprek, J. Vac. Sci. Technol., A, Vac. Surf. Films 17 (1999) 2401.
- [15] S. Veprek, M. Jilek, Pure Appl. Chem. 74 (2002) 475.
- [16] S. Reich, H. Suhr, K. Hanko, L. Szepes, Adv. Mater. 4 (1992) 650.
- [17] J. Castaing, P. Costa, Properties and Uses of Diborides, Springer-Verlag, 1977.
- [18] R. Kieffer, F. Benesovsky, Hartstoffe, Springer-Verlag, 1963.
- [19] M. Mukaida, T. Goto, T. Hirai, J. Mater. Sci. 26 (1991) 6613.
- [20] B.N. Beckloff, W.J. Lackey, J. Am. Ceram. Soc. 82 (1999) 503.
- [21] H.O. Pierson, A.W. Mullendore, Thin Solid Films 95 (1982) 99.
- [22] J. Patscheider, S.Z. Li, S. Veprek, Plasma Chem. Plasma Process. 16 (1996) 341.
- [23] S. Veprek, P. Nesladek, A. Niederhofer, F. Glatz, M. Jilek, M. Sima, Surf. Coat. Technol. 109 (1998) 138.
- [24] S. Jayaraman, E.J. Klein, Y. Yang, D.-Y. Kim, G.S. Girolami, J.R. Abelson, Chromium Diboride Thin Films by Low Temperature Chemical Vapor Deposition, J. Vac. Sci. Technol. 23 (4) (2005) 631.
- [25] S. Jayaraman, Y. Yang, D.-Y. Kim, G.S. Girolami, J.R. Abelson, Hafnium Diboride Thin Films by Chemical Vapor Deposition from a Single Source Precursor, J. Vac. Sci. Technol. 23 (2005) 1619.
- [26] B. McCarroll, Rev. Sci. Instrum. 41 (1969) 279.
- [27] W.C. Oliver, G.M. Pharr, J. Mater. Res. 19 (2004) 3.
- [28] W.C. Oliver, G.M. Pharr, J. Mater. Res. 7 (1992) 1564.
- [29] H.S. Seo, T.Y. Lee, J.G. Wen, I. Petrov, J.E. Greene, D. Gall, J. Appl. Phys. 96 (2004) 878.
- [30] J.A. Thornton, J. Vac. Sci. Technol., A, Vac. Surf. Films 4 (1986) 3059.
- [31] C.V. Thompson, Annu. Rev. Mater. Sci. 30 (2000) 159.
- [32] C.V. Thompson, R. Carel, Mater. Sci. Eng., B, Solid-State Mater. Adv. Technol. 32 (1995) 211.
- [33] A.J. Perry, L. Schlapbach, Solid State Commun. 56 (1985) 837.
- [34] R. Trehan, Y. Lifshitz, J.W. Rabalais, J. Vac. Sci. Technol., A, Vac. Surf. Films 8 (1990) 4026.
- [35] A. Leyland, A. Matthews, Surf. Coat. Technol. 177 (2004) 317.